JOURNAL OF CATALYSIS 63, 235–254 (1980)

Aspects of Selective Oxidation and Ammoxidation Mechanisms over Bismuth Molybdate Catalysts

II. Allyl Alcohol as a Probe for the Allylic Intermediate[1]

JAMES D. BURRINGTON, CRAIG T. KARTISEK, AND ROBERT K. GRASSELLI

The Standard Oil Company (Ohio), Research Department, 4440 Warrensville Center Road, Warrensville Heights, Ohio 44128

Received June 21, 1979; revised November 14, 1979

The oxidation and ammoxidation of allyl alcohol over MoO_3, $Bi_2O_3 \cdot nMoO_3$ ($n = 0, 1, 3$), and a multicomponent catalyst ($M_a^{2+}M_b^{3+}Bi_xMo_yO_z$) have been studied as a method of generating σ-allyl complexes analogous to those formed in the selective oxidation of propylene to acrolein. Adsorption experiments and studies using allyl alcohol-1,1-d_2 and -3,3-d_2 reveal the role of acid/ether-forming sites and oxidation/acrolein-forming sites in the equilibration of C-1 and C-3 of allyl alcohol, and establish hydrogen abstraction as the rate-determining step with $k_H/k_D \cong 2.5$ (320°C, oxidation) and 2.1 (430°C, ammoxidation). Relative product distributions for the catalysts studied show the importance of bismuth in the rate enhancement of the hydrogen abstraction step. These results are interpreted in terms of a selective propylene oxidation mechanism in which the initially formed π-complex collapses to an O σ-complex prior to the second hydrogen abstraction to form reduced catalyst and acrolein. In ammoxidation, the analogous N σ-complex undergoes two hydrogen abstractions to produce acrylonitrile.

INTRODUCTION

The mechanism of selective catalytic oxidation of propylene has been the topic of much study which has recently been reviewed (*1*). These studies, which include analyses of product distribution, kinetics of oxidation of ^2H- and ^{13}C-labeled propylenes (*2*), and the reaction of propylene in the presence of $^{18}O_2$ (*3, 4*) and ^{18}O-labeled catalyst (*5*), have provided much information concerning the rate-determining step (the formation of an allylic intermediate) and the mechanism of oxygen incorporation (Mars–vanKrevelen mechanism of bulk diffusion) (*6*) but relatively little concerning the subsequent steps involved in the formation of selective oxidation products. It is generally accepted that α-hydrogen abstraction from propylene occurs in the rate-determining step. However, the nature of this step and of the allylic intermediate itself is less well understood. EPR evidence has suggested the existence of Mo(V) (*7*) and allyl radicals (*8*) as intermediates, while evidence against acrolein (*9*) and allyl alcohol (*4*) as intermediates in acrylonitrile and acrolein formation respectively has been presented.

The subsequent steps involved in the conversion of the allylic intermediate to selective products are even less well understood. The isotopic ratios for acrolein and acrylonitrile derived from experiments using deuterium-labeled propylene (*2*) suggest that the second hydrogen abstraction occurs to form the carbenoid **2** before oxygen insertion, via a π-allyl intermediate (**1**) which has equal probability of removing a hydrogen atom from either end of the allylic moiety (*1*) [Eq. (1)]. In the case of ammoxidation, the carbene-like intermediate undergoes a third hydrogen abstraction from the methylene end and nitrogen insertion to form acrylonitrile [Eq. (1)].

[1] Presented at the Gordon Research Conference, Symposium on Catalysis, New London, New Hampshire, June 29, 1979.

0021-9517/80/050235-20$02.00/0

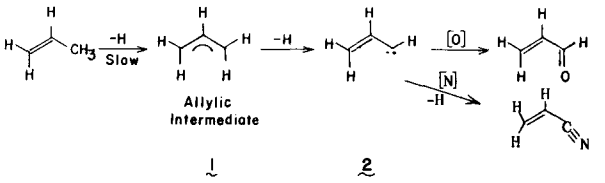

1 2 (1)

Based on relative stabilities of allyl radicals vs carbene it is probable that sequential removal of hydrogens would require more energy for the removal of the second hydrogen (and the third for acrylonitrile formation), an assumption that is consistent with quantum chemical calculations (*9*). However, this conclusion is contrary to experimental evidence, which supports the removal of the first hydrogen to form an allylic intermediate as the rate-determining step.

An alternate mechanism is one in which the oxygen insertion occurs prior to the second α-hydrogen abstraction to form a σ-allyl molybdate **3** either via a π-allyl molybdate **1a** or directly from propylene [Eq. (2)]. The step in which **3** is converted to acrolein,

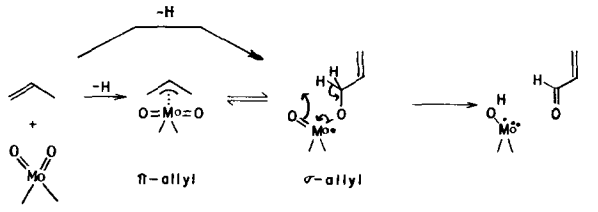

1a 3 (2)

which involves a second α-hydrogen abstraction, is now facilitated by the presence of the C–O bond. Intermediates similar to **3** have been previously proposed (*10*).

Since either end of the allylic fragment in **1a** has equal probability of collapsing on an oxygen, the same isotopic product distribution, based on the known isotope effect, is expected as for the sequential hydrogen removal mechanism, when one starts with propylene deuterated in the 1 or 3 position, provided that **1a** and **3** are in rapid equilibrium with respect to hydrogen abstraction from **3** to form acrolein. This same reasoning applies for ammoxidation by simply replacing the Mo=O moiety with Mo=NH followed by two hydrogen abstractions.

The intermediate **3** may be considered a molybdenum(V) ester. The analogous Mo(VI) ester(**4**), which should be accessible via condensation of allyl alcohol with MoO_3, contains the Mo=O necessary to effect hydrogen abstraction and should thus be a good model for **3** [Eq. (3)]. The importance of metal–oxygen double bonds in catalytic oxidation has been discussed (*11*).

A structure similar to **4** has been observed spectroscopically as a surface inter-

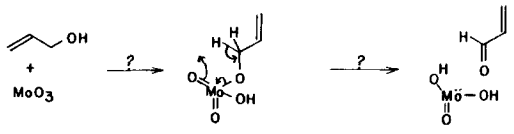

4 (3)

mediate in the selective oxidation of propylene with Mo-containing catalysts (*12a*). The formation of esters of molybdic acid has been proposed in the reaction of alcohols with silica-fixed MoO_3 (*12b*).

Likewise, the analogous esters **5** and **6** formed from the reaction of allyl alcohol with $Bi_2O_3 \cdot MoO_3$ and $Bi_2O_3 \cdot 3MoO_3$ (γ- and α-bismuth molybdate, respectively) may also be studied [Eqs. (4) and (5)].

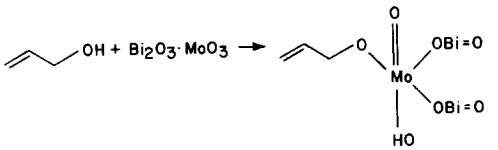

(4)

5

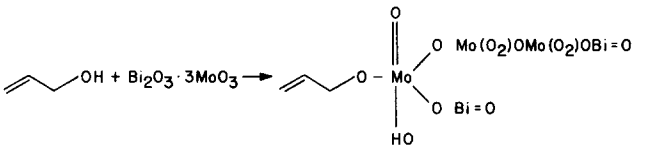

(5)

6

A study of the relative reactivity and product distribution resulting from reaction of these σ-allyl molybdates will provide a theoretical basis for the differences observed in the oxidation and ammoxidation over the various bismuth molybdates and the function of the atomic components of each.

In this work, we have studied in detail the reaction of allyl alcohol with molybdenum trioxide, bismuth(III) oxide, α- and γ-bismuth molybdate, and a multicomponent system. Evidence for the formation of σ-allyl molybdates **4**, **5**, and **6** and conclusions concerning their mechanisms of reaction and relation to the selective oxidation and ammoxidation of propylene will be presented. These conclusions are based on product distributions, adsorption studies, and a study of the reactions of ^{18}O-allyl alcohol and allyl alcohol-1,1-d_2 and -3,3-d_2 with these catalysts.

It should be noted at the outset that it is not our contention that desorbed allyl alcohol is an intermediate in the catalytic oxidation of propylene (*4*). Its use in this study is only as a probe for the *in situ* generation of σ-complexes analogous to those formed in propylene oxidation, for the purpose of gaining mechanistic information concerning those steps after the rate-determining allylic hydrogen abstraction.

EXPERIMENTAL

General

All experiments were performed by the pulse method using the microreactor gas chromatograph system described previously (*13*). Proton nuclear magnetic resonance spectra (NMR) were recorded on a Varian EM 390 (90 MHz) interfaced with a Nicolet 1180 computer. Signals are reported in parts per million downfield from tetramethylsilane with the following notations: s, singlet; d, doublet; t, triplet; q, quartet; m, multiplet, br, broad.

Mass spectra were recorded using a Finnigan 4000 glc/ms system equipped with a Carbowax 20M 100-ft SCOT (support coated open tube) capillary column. Ionizing voltage and column temperature were 10.7 eV, 50°C and 13.7 eV, 80°C for acrolein and acrylonitrile, respectively.

Infrared spectra were recorded on a Nicolet 7199 Fourier Transformer instrument.

Gas–liquid partition chromatography (glc) analyses and separations employed a Varian 3760 (flame ionization or thermal conductivity, helium) using either a Houdry system described previously for pulse reactor work (*13*) or a 6-ft × 1/8-in. stainless-steel column packed with 5% Carbowax 20 M on Anakom SD 80/100 mesh, with a flow rate of 30 cm^3 min^{-1} at 90°C column temperature, for analysis of the prepared labeled compounds. Unlabeled allyl alcohol (MCB, 98+%) was used without further purification.

Preparation of unsupported fixed-bed (20–35 mesh) MoO_3, $Bi_2O_3 \cdot 3MoO_3$ and $Bi_2O_3 \cdot MoO_3$, Bi_2O_3 (*13*), and $M_a^{2+}M_b^{3+}Bi_xMo_yO_z$ (*14*) has been described.

Relevant catalyst properties are shown in Table 1. Catalysts used in all experiments were 100% active phase.

Allyl alcohol-3,3-d_2 was prepared by the method of McMichael (*15*) in two steps from propargyl alcohol. Repeated equilibration of propargyl alcohol with D_2O (SIC, 99.8 atom% D) containing BaO resulted in 88.7 and 92.2% deuterium exchange at the acetylenic (t, 2.39δ) and hydroxyl position (brs, 3.00δ) respectively by NMR ($CDCl_3$) integration compared to methylene group (s, 4.13δ). Reduction of this mixture with $LiAlH_4$ in ether with D_2O workup gave, after microspinning band distillation, a mixture of allyl alcohols [>96% pure (by glc), 10% yield from propargyl alcohol]: 3,3-d_2 (77.3%), 2,3-d_2 (8.9%), 3-d (13.4%), 2-d (0.1%) d_0 (0.4%), 86.4% OH, by NMR ($CDCl_3$) from relative integration of the vinyl methylene (m, 4.97–5.23δ), methine (m, 5.77–5.97δ), methylene (d of d, 4.03δ), and OH (t, 2.20δ) proton signals. This mixture will be referred to as allyl alcohol (77% 3,3-d_2).

TABLE 1

Catalyst Properties

Catalyst	Density (g/cm^3)	S.A. (m^2/g)	Rel. acidity[a]
MoO_3	1.8	0.7	3.0
$Bi_2O_3 \cdot 3MoO_3$	0.79	1.7	2.3
$Bi_2O_3 \cdot MoO_3$	1.0	2.2	1.2
Bi_2O_3	4.4	0.2	0.1
$M_a^{2+}M_b^{3+}Bi_xMo_yO_z$		4.7	2.9

[a] μmole of NH_3 irreversibly adsorbed when a 0.9-cm^3 pulse of 19% NH_3, 81% He (7 μmole NH_3) is passed over 3.92 m^2 of catalyst at 200°C, 3-sec contact time.

Conversion to the trimethylsilyl ether was accomplished by warming a mixture of 20 μl pyridine, 10 μl of the allyl alcohol (77% 3,3-d_2) from above, and 1 μl bis-trimethylsilyltrifluoroacetamide (BTSTA, Regisil, Regis Chemical Co.) at 80°C for 1 hr in a stoppered tube. The mass spectrum of the glc peak corresponding to allyl trimethylsilyl ether gave a $d_2 : d_1 : d_0$ ratio (as measured by the M-15 peaks, 117 : 116 : 115) of 86.5 : 13.5 : 0. (ratio from NMR = 86.2 : 13.5 : 0.4.)

Allyl alcohol-1,1-d_2 was prepared by the method of Schuetz and Millard (*16*) by the reduction of acrylyl chloride (Aldrich, 98%) with lithium aluminum deuteride (ICN) in 22% isolated yield after microspinning band distillation [>97% pure by glc (Flame Ionization Dectector)]; NMR ($CDCl_3$) showed >98% 1,1-d_2, and ~21 mole% water, confirmed by glc using a thermal conductivity detector. This alcohol was converted to the trimethylsilyl ether and analyzed by mass spectroscopy as before to give a $d_2 : d_1 : d_0$ ratio of 98.2 : 1.8 : 0.

Allyl alcohol-1,1-d_2 and -3,3-d_2 (55 : 45 mixture of allyl alcohol-1,1-d_2 : 3,3-d_2) was prepared by isomerization (300°C, 25 min) of the allyl trifluroacetate resulting from the reaction of allyl alcohol-1,1-d_2 and trifluroacetic anhydride with subsequent hydrolysis at 110°C.

^{18}O-Allyl alcohol was prepared by a modification of the method of Murty and Curl (*17*). To a mixture of acrolein dimethyl acetal (8.1 g, 79.4 mmole) and $H_2{}^{18}O$ (2.0 g, 100 mmole, Prochem/Isotopes, 99.0 atom% ^{18}O) was added one drop of concentrated sulfuric acid cautiously and the re-

sulting pale-yellow solution distilled. The fraction boiling at 50–56°C was collected in 10 ml dry ether at 0°C to which had been added a few crystals of hydroquinone. To a stirred suspension of lithium aluminum hydride (1.0 g, 28.5 mmole) in 30 ml dry ether, cooled in an ice–salt bath, was added the above ether solution of ^{18}O-acrolein over 1 hr under an argon atmosphere. The temperature was maintained between 5 and 10°C during the addition. After completion of the addition, the reaction mixture was stirred at 0°C for 30 min, the ice bath removed, and 3 ml of a 15% NaOH solution added slowly. The mixture was allowed to stir for 10 min, at which time a white granular precipitate formed. The mixture was then filtered, the precipitate washed with ether (5 × 10 ml), the resulting ether extract dried (Na_2SO_4), filtered, concentrated to ~6 ml on a rotary evaporator, and the resulting solution distilled on a 24-cm microspinning band column. The fraction boiling at 89–90°C (1.03 g, 22% from acrolein dimethyl acetal) contained >97% allyl alcohol by glc; NMR and ir were also consistent with allyl alcohol; mass spectrum (70 eV) showed ^{18}O : ^{16}O ratio (*m/e* 60 : 58) of 96.3 : 3.7.

Attempted synthesis by the reaction of allyl iodide with H_2O in the presence of silver nitrate gave allyl nitrate as the major product.

Oxidation of unlabeled allyl alcohol is shown in Figs. 1 and 2. The effect of gaseous oxygen in allyl alcohol oxidation and relative product distributions from *n*-propanol and allyl alcohol oxidations are shown in Table 2 and 3, respectively.

Allyl alcohol ammoxidation and allyl amine oxidation are shown in Figs. 5 and 6, respectively.

Effect of diluent on product distribution for the reaction of allyl alcohol with MoO_3 and $Bi_2O_3 \cdot MoO_3$ is shown in Table 6.

Adsorption studies for allyl alcohol and pyridine were performed by following the amount of adsorption vs gas-phase mole fraction when samples of alcohol or pyridine in *n*-octane were pulsed over MoO_3 (0.5 cm^3, 0.98 g, 0.7 m^2) at 135°C, 1-sec contact time, using a constant gas-phase pulse size. Adsorption of allyl alcohol in pyridine was performed by this same method, substituting pyridine for *n*-octane in the above adsorption experiments. Further experimental details and the results of these experiments are given in Fig. 3.

Isotopic Experiments

Allyl alcohol (98% 1,1-d_2 or 77% 3,3-d_2) neat, or in octane, pyridine, or 2-methoxy pyridine for oxidation (320°C) or 3 *M* in 28% ammonium hydroxide solution for ammoxidation (430°C), was injected over MoO_3 and $Bi_2O \cdot 3MoO_3$ and the peaks corresponding to acrolein or acrylonitrile, and allyl alcohol were collected in dry-ice-cooled capillary tubes for NMR or mass spectral analysis. Experimental details and results are shown in Tables 5, 7, 8, and 9. A control experiment using a reactor filled with fused quartz showed that no thermal isomerization of allyl alcohol-1,1-d_2, or that resulting from glc analysis, was occurring.

Reaction of ^{18}O-allyl alcohol and $Mo^{16}O_3$ at 320°C was studied as a function of pulse time (Fig. 4) and diluent (Table 10).

Relative rates of reaction of unlabeled and allyl alcohol (98% 1,1-d_2) over MoO_3 and $Bi_2O_3 \cdot 3MoO_3$ were determined at 320°C, at a constant surface area (0.7 m^2) and 0.25-sec contact time by consecutive injections of each under the same reaction conditions. Results are shown in Table 4.

RESULTS

1. *Yields vs Allyl Alcohol Concentration for MoO_3 and $Bi_2O_3 \cdot 3MoO_3$*

(*a*) *MoO_3* (Fig. 1). As is known from literature studies (*4*) the oxidation of allyl alcohol over MoO_3 gives acrolein in high yield. In this work, the reaction of allyl alcohol in aqueous solution with MoO_3 at 320°C as a function of mole percent in the gas phase shows a very high conversion to acrolein (95%) at low allyl alcohol concentration. Upon increasing the alcohol con-

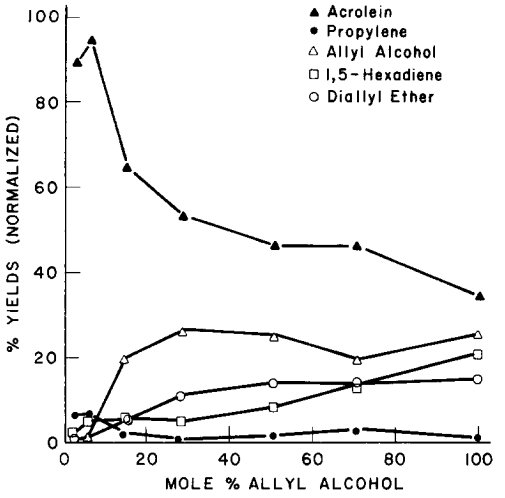

FIG. 1. Yields vs allyl alcohol mole percent for reaction with MoO_3 at 320°C. 0.98 g (0.5 cm^3, 0.7 m^2) MoO_3, 0.25 sec. Catalyst oxidized under air stream at 450°C for 30 min between runs. Pulse size = 1.7 cm^3 (35 μmole allyl alcohol + water).

centration, the yield of acrolein drops due to lower conversion of alcohol and formation of diallyl ether, a dehydration product, and propylene and 1,5-hexadiene which are the $2e^-$ and $1e^-$ reduction products, respectively, of allyl alcohol. This suggests that the formation of propylene and 1,5-hexadiene reflects a $2e^-$ and $1e^-$ reoxidation of surface reduced sites. While the yields of diene and ether increase with increasing alcohol mole percent, the 1,5-hexadiene yield increases much faster at higher concentrations, suggesting a higher order in allyl alcohol for the rate of formation of diene than for that of ether.

(*b*) $Bi_2O_3 \cdot 3MoO_3$ (Fig. 2). As for the MoO_3, a high conversion to acrolein occurs at low allyl alcohol concentrations. However, the yield of propylene is much greater than for MoO_3. This reflects the greater ease of reoxidation of reduced sites for α-bismuth molybdate than for MoO_3 (*18*). The increase in propylene yield with mole percent alcohol injected suggests a higher order dependence on alcohol concentration than for acrolein formation. The dependence of acrolein and diene yield on concentration is similar to that for MoO_3 but less diene is formed since many more of the reduced sites are reoxidized via propylene formation. The low ether yield when compared to MoO_3 reflects the lower surface acidity of α-bismuth molybdate in effecting this dehydration reaction.

The addition of gaseous oxygen to the pulse results in a large increase in acrolein selectivity mainly due to decrease in propylene yield (Table 2). This is probably due to reaction of active surface oxygen rather than lattice oxygen, as has been seen by other workers at this temperature (320°C) (*4*).

The rate of formation of propionaldehyde from *n*-propanol is about five times slower than that of acrolein from allyl alcohol (Table 3). Thus, the double bond enhances but is not necessary for oxydehydrogenation.

2. *Relative Rates of Reaction of Allyl Alcohol-d_0 and -1,1-d_2 over MoO_3 and $Bi_2O_3 \cdot 3MoO_3$*

In order to ascertain the nature of the rate-determining step in this reaction, we have measured the relative rate of oxida-

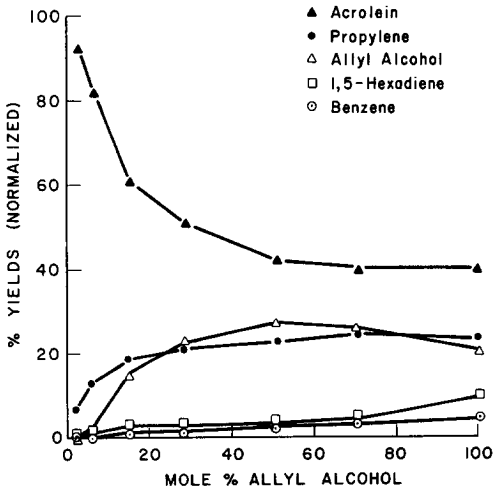

FIG. 2. Yields vs allyl alcohol mole percent for reaction with $Bi_2O_3 \cdot 3MoO_3$ at 320°C. 0.4 g (0.5 cm^3, 0.7 m^2) $Bi_2O_3 \cdot 3MoO_3$, 0.25 sec. Catalyst reoxidized under air at 450°C, 30 min between runs. Pulse size = 1.7 cm^3 (35 μmole allyl alcohol + water).

TABLE 2

Comparison of Reactions of Allyl Alcohol with $Bi_2O_3 \cdot 3MoO_3$ in the Presence and Absence of O_2, 320°C[a]

Conditions	Percentage conversion of AA	Percentage yields (normalized)						
		CO_2	$C_3^=$	Acrolein	HD	PhH	AE	C bal.
Without O_2[b]	91.87	0.04	28.78	55.66	5.79	0.63	0.97	103.8
With O_2[c]	94.97	2.70	3.92	86.82	0.89	—	0.64	103.3

[a] 0.5 cm^3 (0.4 g, 0.7 m^2) $Bi_2O_3 \cdot 3MoO_3$, 0.25-sec contact time; AA = allyl alcohol, HD = 1,5-hexadiene, AE = diallyl ether, PhH = benzene.

[b] 12.1 μmole allyl alcohol per pulse (0.9 μl of 13.4 *Maq*).

[c] 12.1 μmole allyl alcohol + 36.9 μmole O_2.

tion of allyl alcohol-1,1-d_2 and unlabeled allyl alcohol.

The results (Table 4) indicate a faster rate of both overall reaction and acrolein formation for allyl alcohol-d_0 than for allyl alcohol-1,1-d_2 ($kd_0/kd_2 = 1.2$). This result reflects a dilution of the true isotope effect [k_H/k_D (max, 320°C) = 2.5] by formation of products which involve no C–H (D) bond breaking (ether, diene, propylene). This low kd_0/kd_2 also results, in part, from equilibration of the two terminal carbons of allyl alcohol 1,1-d_2 to form allyl alcohol-3,3-d_2 along with oxidation to both acrolein-1-d and acrolein-3,3-d_2 as discussed below in the section on oxidation of allyl alcohol-1-1-d_2 and -3,3-d_2.

This indicates that the rate-determining step in the selective oxidation of allyl alcohol is allylic hydrogen abstraction to form acrolein which corresponds to the fast second hydrogen abstraction in propylene oxidation. Thus, information concerning the role of the elemental components of the catalyst in this second hydrogen abstraction step can be obtained by a comparison of the reactions of allyl alcohol with catalysts of varying composition, discussed in the next section.

3. *Comparison of MoO_3 and $Bi_2O_3 \cdot nMoO_3$ ($n = 3, 1, 0$)*

Table 5 shows the relative product yields in the reaction of allyl alcohol with the five catalysts studied, namely, MoO_3, α- and γ-bismuth molybdate, Bi_2O_3, and a multicomponent (MC) system at 320°C. The order of decreasing activity and decreasing conversion to acrolein in this series follows the order MC > γ > α > MoO_3 > Bi_2O_3. In the MoO_3/bismuth molybdate series, the successive introduction of bismuth into the molybdate esters formed facilitates the abstraction of hydrogen in the rate-determining step to form acrolein.

Bismuth oxide, however, is very inactive because it lacks the chemisorption site for

TABLE 3

Comparison of Reactions of Allyl Alcohol[a] and *n*-Propanol[a] over MoO_3 (320°C)[b]

Starting alcohol	Percentage conversion of alcohol	Percentage yields (normalized)				
		$C_3^=$	Aldehyde (k)	Ether	1,5-Hexadiene	Benzene
n-Propanol	20.1	10.6	7.6 (1.0)	2.0	—	—
Allyl alcohol	72.0	3.1	33.9 (5.2)	14.0	18.7	2.3

[a] 10.4 μmole per pulse, injected neat.

[b] 0.5 sec (0.98 g, 0.7 m^2), 0.25-sec contact time.

TABLE 4

Product Distributions for Reaction of Allyl Alcohol-d_0 and -1,1-d_2 over MoO_3 and $Bi_2O_3 \cdot 3MoO_3$ at 320°C, 0.25 sec, 0.7 m^2[a]

Catalyst	Allyl alcohol	AA	Acrolein	$C_3^=$	HD	PhH	AE	Selectivity to acrolein	kd_0/kd_2
MoO_3	d_0	53.9	28.7	0.6	7.8	0.7	8.4	62.2	1.22
	1,1-d_2[b]	60.2	21.9	0.5	6.6	0.8	10.1	55.0	
$Bi_2O_3 \cdot 3MoO_3$	d_0[c]	31.1	41.2	16.8	7.6	2.1	1.1	59.8	1.19
	1,1-d_2[d]	37.6	35.7	15.6	7.4	2.3	1.5	57.2	

[a] 1.3 μl of 13.4 *M* injected per pulse, AA = allyl alcohol, HD = 1,5-hexadiene, AE = diallyl ether, PhH = benzene.
[b] Average of 4 runs.
[c] Average of 2 runs.
[d] Average of 3 runs.

the allyl molbydate formation, while in the multicomponent system, both bismuth and other di- and trivalent metals facilitate this hydrogen abstraction.

Thus, since the molybdate ester is formed in a fast step, these results show that bismuth is the critical element in facilitating the hydrogen abstraction from the molybdate intermediate, as long as enough Mo is present to allow fast formation of the allyl molybdate.

The analagous results for propylene oxidation (*13*) show that the relative rates for simple bismuth molybdates are in decreasing order, $\beta \approx \alpha > \gamma > MoO_3 \sim Bi_2O_3$. This is consistent with a rate-determining step which requires activation of propylene by both chemisorption on Mo centers and hydrogen abstraction on Bi centers. The γ-phase and Bi_2O_3 have too few chemisorption sites while MoO_3 has no α-hydrogen abstracting sites, and thus these catalysts are less active. The α- and β-phases are the most active and selective catalysts of the simple Bi/Mo series since they have a favorable balance of the two sites necessary to effect the rate-determining first hydrogen abstraction.

The formation of ether and propylene, as stated earlier, reflects the catalyst's acidity and its ease of reduction, respectively. Thus, the multicomponent system is both the easiest to be reduced and to be reoxidized by allyl alcohol, while MoO_3 has the highest and Bi_2O_3 the lowest surface acidity. (See Table 1.)

The yield of products does not change drastically with pulse number for any of the

TABLE 5

Product and Isotopic Distribution from Allyl Alcohol-1,1-d_2 Oxidation (Low Conversion)[a]

Catalyst	cm^3 catalyst	Percentage yields (normalized)[b]							Acrolein (%)[c]		AA (%)[c]	
		CO_2	$C_3^=$	Acrolein	AA	HD	PhH	AE	1-d_1	3,3-d_2	1,1-d_2	3,3-d_2
MoO_3	0.5	Trace	2.0	13.3	64.0	4.1	0.7	15.9	40.6	59.3	58.9	41.1
$Bi_2O_3 \cdot 3MoO_3$	0.5	Trace	17.4	29.5	42.3	7.2	2.0	1.4	47.1	52.9	77.0	23.0
$Bi_2O_3 \cdot MoO_3$	0.32	Trace	21.5	38.9	33.2	4.7	0.9	0.9	44.1	55.9	74.0	26.0
Bi_2O_3	0.8	0.2	1.7	13.2	80.4	3.8	—	0.7	82.1	17.9	90.9	9.1
$M_a^{2+}M_b^{3+}Bi_xMo_yO_z$	0.17	—	21.5	49.8	19.3	4.0	0.8	4.5	35.1	64.9	58.3	41.7

[a] 0.25-sec contact time, 0.7 m^2 total surface area, 42 μmole (3 μl neat allyl alcohol) injected, 320°C.
[b] AA = allyl alcohol, HD = 1,5-hexadiene, AE = diallyl ether, PhH = benzene.
[c] Ratios by NMR.

catalysts, despite the fact that MoO_3 makes very little propylene, whereas $Bi_2O_3 \cdot 3MoO_3$ and $Bi_2O_3 \cdot MoO_3$ make a considerable amount. Thus, the bulk diffusion of lattice oxygen to reduced sites must be fast enough in all of these catalysts to keep up with each two-electron oxidation of allyl alcohol to acrolein and benzene. Since the relative rates of reoxidation by O_2 (lattice mobility) decrease in the order $Bi_2O_3 \cdot MoO_3 > Bi_2O_3 \cdot 3MoO_3 > MoO_3$ (*18*), the rapid reconstruction of reduced catalytic sites is much faster than the rate-determining step (hydrogen abstraction) in these reactions.

4. Effect of Diluent

The effect of diluent on product distribution for the reaction of allyl alcohol with MoO_3 and α-bismuth molybdate at 320°C reveals some important features of the mechanism of this reaction (Table 6). For both these catalysts, a comparison of the reaction using water or pyridine bases with that using an inert diluent, *n*-octane, was obtained.

For MoO_3, the reaction using water as diluent gives slightly less acrolein yield, but much less converison due to a smaller yield of reduced products, propylene and 1,5-hexadiene. When the diluent is pyridine or 2-methoxypyridine, the ether and propylene yields are reduced to nearly zero, while the acrolein yield remains unchanged. For α-bismuth molybdate, the same general trends are seen, except that ether yields are very low regardless of solvent, due to its lower surface acidity compared to MoO_3.

Several important mechanistic conclusions follow from these results. First, since acrolein yield is insensitive to base, acid sites are not involved in the formation of acrolein. However, the dehydration of allyl alcohol to form diallyl ether is occurring on acid sites, since its formation is drastically reduced on addition of base. In addition, propylene is probably formed from reduced acid sites, a process which is inhibited by pyridine.

These results suggest that two types of sites are involved in the reaction of allyl alcohol with MoO_3 and bismuth molybdate, namely, acid sites, which are involved in ether formation, and oxidizing sites, on which acrolein is formed. In order to gain more information concerning the relative number of these sites, low-temperature adsorption studies were performed, discussed in the following section.

5. Adsorption Experiments

Adsorption studies were performed at

TABLE 6

Diluent Effect on Product Distribution from Allyl Alcohol + MoO_3 and $Bi_2O_3 \cdot 3MoO_3$, 320°C[a]

	Diluent[d]	Percentage yields						Percentage acrolein selectivity
		$C_3^=$	Acrolein	AA	HD	PhH	AE	
(1) MoO_3[b]	*n*-Octane	6.4	66.0	3.8	15.4	1.4	7.0	68.6
	H_2O	0.8	61.7	24.1	3.5	0.8	9.0	81.3
	Pyr	0.1	67.6	20.7	10.8	0.5	—	85.2
	2-MPyr	1.5	63.2	22.7	12.1	TR	0.3	85.2
(2) $Bi_2O_3 \cdot 3MoO_3$[c]	*n*-Octane	27.1	63.0	0.7	5.0	3.8	0.4	63.4
	H_2O	21.8	60.9	11.3	3.6	2.2	0.3	68.7
	Pyr	20.3	64.2	10.3	4.8	0.4	—	71.6

[a] All experiments: vapor phase feed = 5.8 μmole allyl alcohol, 15.1 μmole diluent; 0.7 m^2 catalyst; 0.25-sec contact time; AA = allyl alcohol, HD = 1,5-hexadiene, AE = diallyl ether, PhH = benzene.

[b] 0.5 cm^3 (0.98 g) MoO_3.

[c] 0.5 cm^3 (0.4 g) $Bi_2O_3 \cdot 3MoO_3$.

[d] Pyr = pyridine; 2-MPyr = 2-methoxy pyridine.

135°C by increasing the mole fraction of allyl alcohol in *n*-octane and measuring the amount of alcohol in the effluent, using the pulse apparatus described previously. These experiments (squares, Fig. 3) gave a site density of about 2.0×10^{18} sites/m^2. The corresponding experiments for pyridine adsorption (triangles) gave an acid site density of 1.5×10^{18} sites/m^2. A series of experiments were then performed in which the alcohol adsorption was measured as a function of gas-phase mole percent of alcohol in pyridine. This curve (circles) shows an inflection point corresponding to 0.7×10^{18} molecules/m^2.

These results are consistent with a dual-site structure for MoO_3 in which the total number of alcohol chemisorption sites (2×10^{18}/m^2) is composed of acrolein-forming sites (7×10^{17}/m^2) on which allyl alcohol is chemisorbed exclusively in the presence of excess pyridine, represented by the portion of the curve (Fig. 3) to the left of inflection, and about twice as many acid sites (1.5×10^{18}/m^2) on which allyl alcohol is chemisorbed in the region of lower pyridine concentration, to the right of inflection.

6. *Oxidation and Ammoxidation of Allyl Alcohol-1,1-d_2 and -3,3-d_2*

In this study, we are mainly concerned with the reaction of allyl alcohol on acrolein-forming sites to form the allyl molybdate intermediate. Thus, our experiments using deuterated allyl alcohols, which will determine the feasibility of our proposed allyl molybdate intermediate (analogous to **4**), must be interpreted in terms of the reaction which occurs on acrolein-forming sites.

(*a*) *Reactions in the absence of base.* The reactions observed here are a composite of those occurring on acid and acrolein-forming sites.

The acrolein d_1/d_2 ratio observed from oxidation of allyl alcohol-1,1-d_2 or -3,3-d_2 under high conversion conditions (~3 cm^3

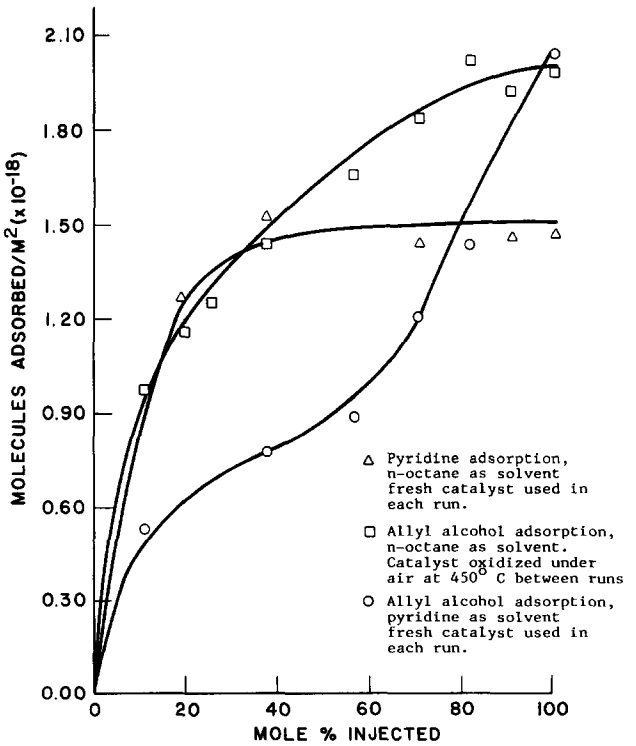

FIG. 3. Adsorption of allyl alcohol and pyridine on MoO_3 at 135°C. 0.9 g (0.5 cm^3, 0.7 m^2) MoO_3 used. Pulse size = 0.35 cm^3 (10.4 μmole total).

TABLE 7

Isotopic Distribution for Products in Oxidation and Ammoxidation of Allyl Alcohol over MoO_3 (2.9 cm^3), 2 sec (High Conversion)

Oxidation (320°C)	Starting alcohol	Products	Experimental %[e]	Theoretical % (Allylic intermediate)[f]	Percentage conversion
	CH_2CHCD_2OH[a]	Acrolein-d_2	69.4[g]	70.1	72.5
		-d_1	30.6[g]	29.7	
		-d_0	0[g]	0.2	
	CD_2CHCH_2OH[b]	Acrolein-d_2	62.1	61.4	75.3
		-d_1	33.3	35.6	
		-d_0	4.6	2.2	
Ammoxidation (430°C)					
	CH_2CHCD_2OH[c]	Acrylonitrile-d_2	68.6	67.4	93.3
		-d_1	1.6	1.6	
		-d_0	29.8	31.0	
	CD_2CHCH_2OH[d]	Acrylonitrile-d_2	61.5	58.1	91.6
		-d_1	12.3	11.6	
		-d_0	26.2	30.4	

[a] 2 μl of 11.8 M alcohol in H_2O per pulse; average of 8 runs.
[b] 2 μl of 14.7 M alcohol in H_2O per pulse; average of 9 runs.
[c] 3.3 μl of 2.7 M alcohol, 10.9 M NH_3 in H_2O; average of 6 runs.
[d] 2 μl of 3 M alcohol, 12 M NH_3 in H_2O; 13.7 eV (AN). Similar runs in H_2O or using 11 μmole of neat allyl alcohol + 37 μmole of anhydrous NH_3 gave similar results.
[e] By mass spectroscopy at 10.7 eV (acrolein), 13.7 eV (AN).
[f] Calculated k_H/k_D (320°C) = 2.5; (430°C) = 2.2.
[g] Analysis by NMR gave a 65.9 : 34.1 : 0 ratio.

catalyst, 2-sec contact time) indicates that total equilibration of C-1 and C-3 of allyl alcohol occurs for MoO_3 in both oxidation and ammoxidation reactions (Table 7) and

TABLE 8

Isotopic Distribution for Products in Oxidation of Allyl Alcohol over $Bi_2O_3 \cdot 3MoO_3$ (3.0 cm^3) at 320°C, 2 sec (High Conversion)

Starting alcohol	Products	Experimental %[a]	Theoretical %		
			Allyl	100% retention	% conv.
CH_2CHCD_2OH[b]	Acrolein-d_2	54.1	70.1	0	97.9
	-d_1	44.3	29.7	99.5	
	-d_0	1.6	0.2	0.5	
	Propylene-d_2 (32.3% conversion)	96.7 (91.0)	100	100	
	-d_1	2.1 (3.0)	0	0	
	-d_0	1.2 (0.4)	0	0	
	-d_3	0 (5.6)	0	0	
CD_2CHCH_2OH[c]	Acrolein-d_2	69.4	61.4	84.5	99.1
	-d_1	30.6	35.6	14.8	
	-d_0	0	2.2	0.5	

[a] By mass spectroscopy at 10.7 eV; numbers in parentheses are for catalyst after 5 pulses.
[b] 2.1 μl of 11.8 M alcohol per pulse; average of 5 pulses.
[c] 2.0 μl of 14.7 M alcohol per pulse; average of 5 pulses.

TABLE 9

Effect of Base on Product and Isotopic Distribution for Reaction of Allyl Alcohol-d_2 and Propylene-d_2 at 320°C[a]

Catalyst	Diluent[c]	AA	Percentage yields[b]							Acrolein (%)[d]		AA (%)[d]	
			AA: solvent	$C_3^=$	Acrolein	AA	HD	PhH	AE	1-d_1	3,3-d_2	1,1-d_2	3,3-d_2
MoO_3	*n*-Octane	1,1-d_2	1.7	4.4	30.1	38.2	7.1	1.5	19.0	41.8	58.2	56.7	43.3
MoO_3	2-MPyr	1,1-d_2	1.7	0.6	27.4	64.5	6.9	0.0	0.8	56.0	44.0	72.2	27.8
MoO_3	Pyr	1,1-d_2	0.4	0.0	48.8	46.5	4.7	0.0	*e*	57.0	43.0	77.3	22.7
$Bi_2O_3 \cdot 3MoO_3$	*n*-Octane	1,1-d_2	1.7	25.1	37.0	30.2	3.8	3.1	0.8	52.0	48.0	73.0	27.0
$Bi_2O_3 \cdot 3MoO_3$	Pyr	1,1-d_2	1.7	19.8	35.1	38.8	4.5	1.3	0.4	69.8	30.2	82.3	17.7
$Bi_2O_3 \cdot 3MoO_3$	Pyr	1,1-d_2	0.4	20.4	44.2	29.5	5.4	0.5	0.0	66.8	33.2	*f*	*f*
$Bi_2O_3 \cdot 3MoO_3$	Pyr	1,1/3,3-d_2[g]	0.4	26.9	54.0	10.3	8.9	0.0	0.0	31.6	68.4	*f*	*f*
$Bi_2O_3 \cdot 3MoO_3$	Pyr	1,1/3,3-d_2[g,h]	0.4	6.0	20.0	70.4	3.6	0.0	0.0	*f*	*f*	55.7	44.3
$Bi_2O_3 \cdot 3MoO_3$	—	$C_3^=$–1,1-d_2[i]	—	91.5	8.5	0.0	0.0	0.0	0.0	29.4	70.6	—	—

[a] 0.25-sec contact time, 0.7 m² catalyst, AA + solvent = 32 μmole total, unless otherwise stated.
[b] $C_3^=$ = propylene, AA = allyl alcohol, HD = 1,5-hexadiene, PhH = benzene, AE = diallyl ether.
[c] 2-MPyr = 2-methoxy pyridine, Pyr = pyridine.
[d] Ratios by NMR.
[e] Masked by pyridine peak.
[f] Not enough collected to analyze by NMR.
[g] 55:45 (1,1-d_2:3,3-d_2) mixture used.
[h] Contact time = 0.025 sec, 0.07 m² catalyst.
[i] Feed = 24.5 μmole C_3^{2-}–1,1-d_2; 3.0 cm³ (2.48 g, 4.2 m²) $Bi_2O_3 \cdot 3MoO_3$; 15-sec contact time.

fits well the theoretical maximum k_H/k_D [2.51 (320°C), 2.18 (430°C)]. However, for $Bi_2O_3 \cdot 3MoO_3$ (Table 8), there is a net retention of original carbon integrity in the oxidation reaction, i.e., more acrolein-1-*d* is formed from allyl alcohol-1,1-d_2 and more acrolein -3,3-d_2 from the 3,3-d_2 isomer than expected, based on the isotope effect (k_H/k_D = 2.5).

When the reaction of allyl alcohol-1,1-d_2 is run under conditions of low conversion (0.3–0.5 cm³ catalyst, 0.25 sec) for both MoO_3 and $Bi_2O_3 \cdot 3MoO_3$ incomplete isomerization to a mixture of allyl alcohol-1,1-d_2 and -3,3-d_2 occurs, the degree of which decreases in the following order: multicomponent $\approx MoO_3 > Bi_2O_3 \cdot MoO_3 \approx Bi_2O_3 \cdot 3MoO_3 \gg Bi_2O_3$ (Table 4). The 1-*d*:3,3-d_2 ratio of the acrolein isolated reflects an enrichment in the 3,3-d_2 component when compared to the allyl alcohol-3,3-d_2:1,1-d_2 ratio, due to the deuterium isotope effect.

(*b*) *Reactions in the presence of base.* In order to distinguish between acid-site and oxidizing-site isomerization, the effect of base on the isotopic distribution in the acrolein and unoxidized alcohol resulting from the reaction of allyl alcohol-1,1-d_2 at 320°C over MoO_3 and α-bismuth molybdate was investigated. The results in Table 9 show that for these catalysts, less isomerization to allyl alcohol-3,3-d_2 and, correspondingly, less acrolein-3,3-d_2 formation occur when the reaction is run in the presence of sufficient base to eliminate acid sites. The fact that a substantial portion of the isomerization occurs in the presence of excess base indicates that both acid sites and acrolein-forming sites are responsible for interconversion of the two ends of the allylic species.

Several important features of these experiments run in the presence of base, which represent reaction on acrolein-forming sites only, are worthy of note. First of all, the ratio of acrolein-3,3-d_2:1-*d* formed on both catalysts is much less than the 29:71 ratio observed for the reaction of propylene-1,1-d_2 (Table 9) which results from a k_H/k_D isotope effect of 2.4, indicating that total equilibration of the isomeric allyl molybdates is not occurring. However, when compared to the 3,3-d_2:1,1-d_2 ratio in the isolated unoxidized alcohol, the acrolein-3,3-d_2:1-*d* ratio indicates that enough isomerization is occurring to result in an enrichment in the 3,3-d_2 component as expected based on a hydrogen–deuterium iso-

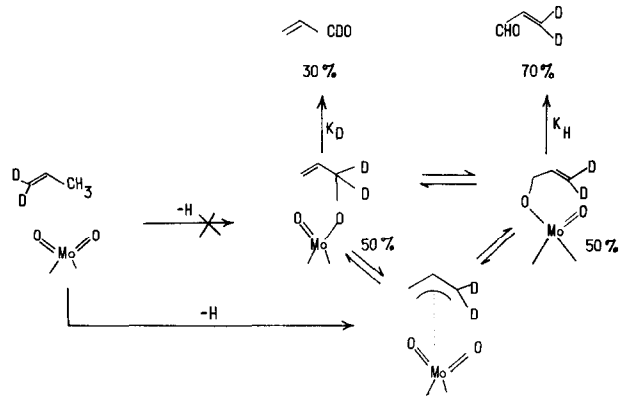

SCHEME 1. Reaction of propylene-1,1-d_2 with molybdate catalysts.

tope effect of about 2.4. Furthermore, if one starts with a 1 : 1 mixture of allyl alcohol-1,1-d_2 and -3,3-d_2, the same ratio of acrolein-3,3-d_2: 1-d is obtained as that observed in the reaction of propylene-1,1-d_2. These isotopic experiments show that there is not enough equilibration to accommodate a mechanism in which the σ O-allyl molybdate is formed directly from propylene, but sufficient equilibration does occur to be consistent with the initial formation of a π-allyl intermediate, followed by formation of either σ O-allyl intermediate in equal amounts and subsequent H or D abstrac-

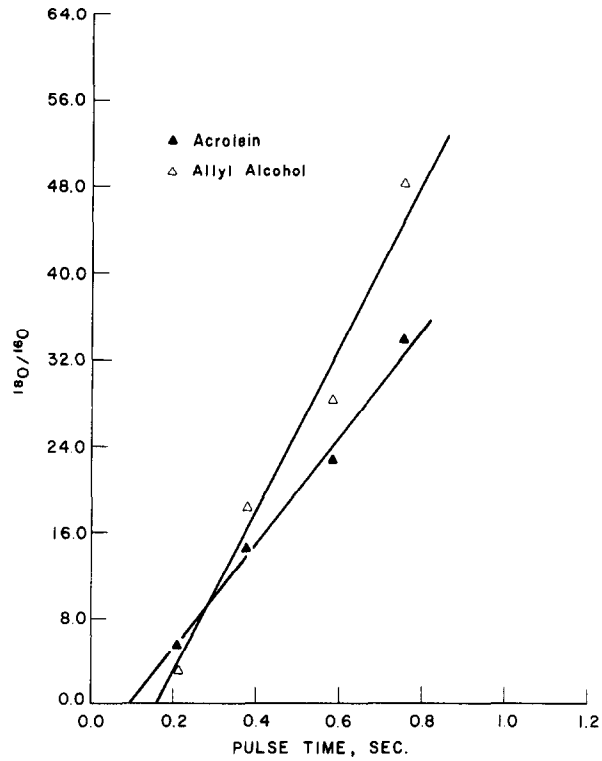

FIG. 4. ^{16}O Incorporation into acrolein and allyl alcohol from reaction of ^{18}O-allyl alcohol with MoO_3 at 320°C. 1.96 g (1.0 cm^3, 1.4 m^2) MoO_3. Fresh catalyst used for each injection. Molar velocity = 83.5 μmole sec^{-1}.

tion to form acrolein-3,3-d_2 and -1-d in the expected ratio based on an isotope effect of 2.4 at 320°C (Scheme 1).

Oxidation of ^{18}O-Allyl Alcohol over $Mo^{16}O_3$

The results in Fig. 4 show that a high degree of ^{16}O incorporation (low $^{18}O/^{16}O$) occurs in both isolated alcohol and acrolein at low pulse times (0.2 sec = 16.7 μmole injected). This incorporation falls off with pulse time, faster for isolated alcohol than for acrolein, indicating that some ^{16}O incorporation must be associated with the path leading to acrolein on selective oxidation sites.

The amount of ^{16}O incorporation into acrolein is insensitive to base, while a basic reaction medium causes much less ^{16}O incorporation in the isolated alcohol (Table 10).

These results support a dual-site mechanism in which ^{16}O incorporation occurs on both acid and acrolein-forming sites, the latter process being insensitive to base.

TABLE 10

Effect of Base on ^{18}O-Allyl Alcohol Oxidation over MoO_3 at 320°C[a]

Diluent	$^{18}O/^{16}O$[b]	
	Acrolein	Allyl alcohol
n-Octane	0.142	0.229
Pyridine	0.123	0.670

[a] 0.25 cm³ (0.49 g) MoO_3 used; 0.06-sec contact time; alcohol : diluent ratio = 0.33, 3.5 μl of 3.2 *M* in alcohol, 9.6 *M* diluent injected.

[b] Ratios by mass spectroscopy.

Ammoxidation–Nitrogen Incorporation Experiments

(*a*) *Yield vs NH_3:allyl alcohol ratio, 380°C (Fig. 5).* Experiments in which the ammonia : allyl alcohol ratio is varied from 0 to 9.2 show that six ammonia molecules

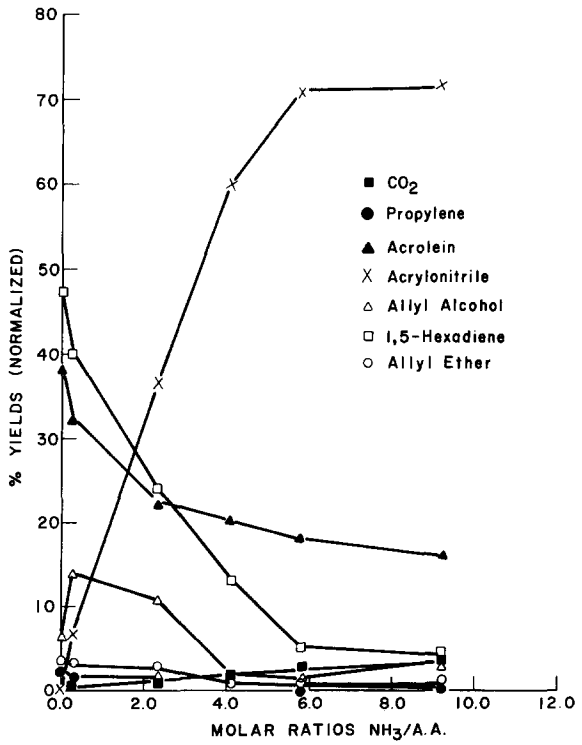

FIG. 5. Yields vs ammonia : allyl alcohol ratio for reaction with MoO_3 at 380°C. AA = allyl alcohol. 0.98 g (0.5 cm³, 0.7 m²) MoO_3 used. Fresh catalyst used for each run. Pulse size = 1.9 cm³ (35 μmole total).

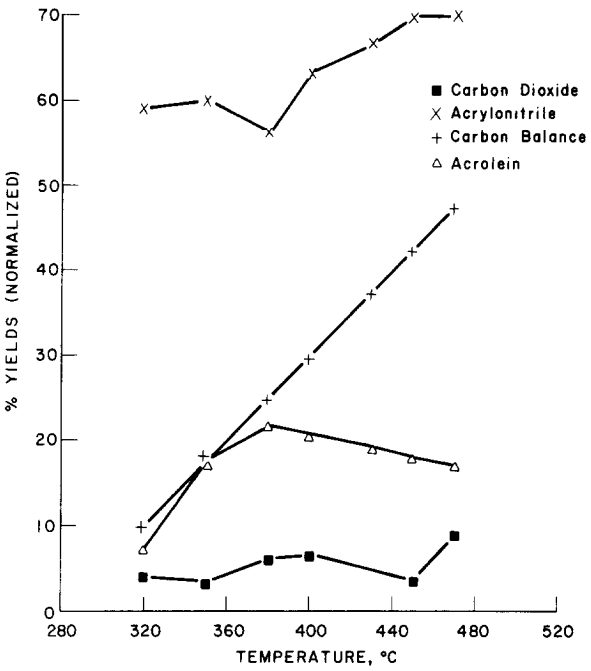

FIG. 6. Yields vs temperature in allyl amine oxidation over MoO_3. 5.4 g (3 cm^3, 3.8 m^2) MoO_3, 2 sec. Catalyst oxidized under air stream 30 min at 450°C between runs. 1 μl of 2.9 *M* allyl amine in H_2O injected at each temperature.

per allyl alcohol in the gas phase are required for maximum acrylonitrile (AN) formation to occur. No ammonia burning was observed in these experiments. Although the relative adsorption coefficients for allyl alcohol and NH_3 are not known, these results suggest that there is a requirement for several ammonia molecules per allyl alcohol on the catalytic site for selective oxidation to achieve maximum AN yield.

(*b*) *Reaction of allyl amine with* MoO_3 (*Fig. 5*). This reaction gave acrylonitrile as the major product, with substantial amounts of acrolein. At 320°C the carbon balance is very low (15%), but increases with increasing temperature. The inability of the active site to undergo the required four-electron reduction and the difficulty of desorption of acrylonitrile at the lower temperature are probably responsible for the low carbon balances. The presence of acrolein suggests that an initially formed N-bonded σ-complex can be converted to an O-bonded σ-complex, which is the acrolein precursor, although hydrolysis of an imine intermediate might also contribute to its formation.

DISCUSSION

The reactions of allyl alcohol with MoO_3, $M_a^{2+}M_b^{3+}Bi_xMo_yO_z$, and $Bi_2O_3 \cdot nMoO_3$ (n = 0, 1, 3) can be divided into two main groups: alcohol isomerization and acrolein/propylene/diene formation. The proposed mechanisms for these processes are depicted in Schemes 2 and 3 for MoO_3.

Allyl Alcohol Isomerization (Scheme 2)

The isomerization reaction, namely, interconversion of allyl alcohol-1,1-d_2 and -3,3-d_2, can be explained on the basis of two effects, namely, carbonium ion formation on acid/ether-forming sites and the interconversion of the isomeric allyl molybdate-1,1-d_2 and -3,3-d_2 (**4**), the acrolein precursors, on acrolein-forming sites. Interaction of allyl alcohol-1,1-d_2 with acid sites, represented in Scheme 2 as surface hydroxyls, results in dehydration to form a chemi-

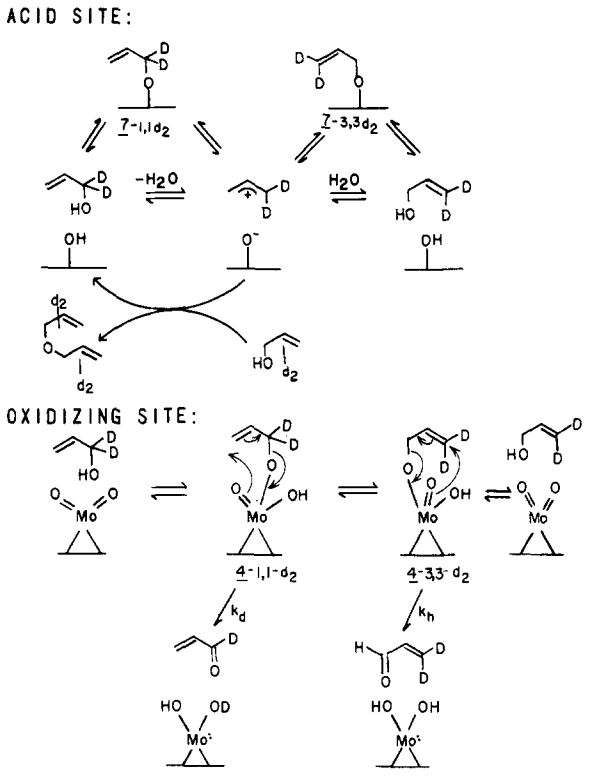

SCHEME 2. Allyl alcohol-1,1-d_2/3,3-d_2 isomerization, ether formation, and oxidation over MoO_3.

sorbed allyl cation, which can either react with another molecule of allyl alcohol to form ether, after loss of a proton, or give isomerized (3,3-d_2) allyl alcohol via 7-3,3-d_2 or starting alcohol (1,1-d_2) via 7-1,1-d_2, or by direct hydration.

Interaction of allyl alcohol with an oxidizing site, represented as surface Mo=O double bonds, gives molybdate ester 4-1,1-d_2, which can undergo rearrangement to 4-3,3-d_2 and subsequently desorb as allyl alcohol-3,3-d_2. The importance of Mo=O double bonds in this process is depicted. Acrolein formation from each of these intermediates occurs with rate constants k_D and k_H, respectively. The equilibration here is not complete at 320°C, but can accommodate a faster C–H bond breaking to give the expected acrolein-3,3-d_2 : 1-d ratio (70 : 30), based on the reaction of propylene-1,1-d_2 (Table 9). The isomerization which occurs in the presence of base is due to interconversion of the σ-allyl molybdates 4-1,1-d_2 and 4-3,3-d_2, either by a Cope-type rearrangement (a formal 3,3-sigmatropic shift) as shown in Scheme 2, or via C–O cleavage to form an allyl/molybdate pair which then reforms the C–O bond on the other terminal carbon. By either path, the importance of the Mo=O is apparent and consistent with the higher degree of isomerization for MoO_3 than $Bi_2O_3 \cdot 3MoO_3$ in the presence of base (27.8% allyl alcohol-3,3-d_2 for MoO_3 vs 17.7% allyl alcohol-3,3-d_2 for $BiO_3 \cdot 3MoO_3$, Table 9).

Acrolein, Propylene, and Dimer Formation (Scheme 3)

The proposed mechanism for these reactions is shown in Scheme 3. Reaction of allyl alcohol with an oxidizing site produces **4**, which upon 1,4-hydrogen transfer results in a two-electron reduction of Mo and production of acrolein.

Propylene formation occurs by the reaction of a reduced acid site with alcohol with dehydration to form **8** followed by dispro-

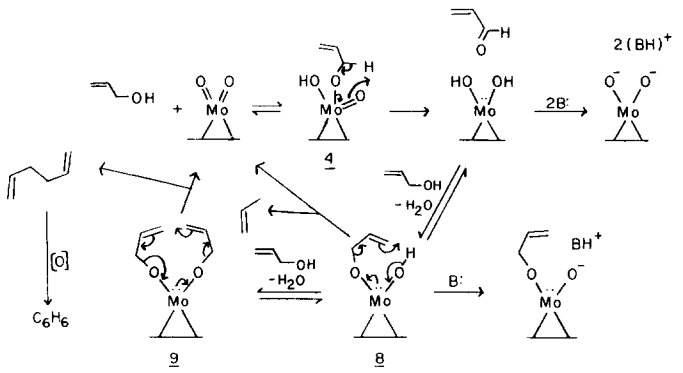

SCHEME 3. Acrolein, propylene, and dimer formation from allyl alcohol over MoO_3.

portionation to regenerate an oxidized site. The 1,5-hexadiene results from further reaction of allyl alcohol with propylene precursor **8** and loss of water to form **9**, which can disproportionate to give 1,5-hexadiene and the oxidized site.

Pyridine inhibits this propylene/diene-forming path by reacting with **8** and the reduced acid site. Inhibition of this path by water results because **8** and **9** are formed from dehydration reactions. The use of water or pyridine has little effect on the acrolein yield although both result in a large decrease in conversion due to a decrease in propylene and diene yields. Thus, only oxidizing and not acid sites are capable of forming the molybdate ester **4**, the acrolein precursor.

The acrolein yield decreases, while the yield of diallyl ether and 1,5-hexadiene increases, upon increasing the initial concentration of allyl alcohol (Figs. 1 and 2). Propylene yield increases initially but then follows a downward trend in this series. The increase in diene yield is faster than that of ether at higher initial alcohol concentrations. This is in accord with the predictions of Schemes 2 and 3 in which the formation of acrolein requires the reaction of only one molecule of allyl alcohol, while that of diallyl ether or propylene requires two molecules and that of 1,5-hexadiene three.

The conversion to acrolein (and total conversion) is decreasing in the order $Bi_2O_3 \cdot MoO_3 > Bi_2O_3 \cdot 3MoO_3 > MoO_3$. Thus, the presence of bismuth atoms at the acrolein-forming chemisorption site (Mo) enhances the rate of allylic hydrogen abstraction either by abstraction of hydrogen via Bi–O bonds or by providing a sink for the molybdenum to which it can transfer electrons after hydrogen abstraction by molybdenum oxygens. The fact that MoO_3 has substantial activity toward oxidizing allyl alcohol to acrolein suggests the latter explanation. The multicomponent system is the most active in this series, due to an enhancement in its ability to be reduced resulting from favorable electronic and structural characteristics.

Ammoxidation of Allyl Alcohol and Oxidation of Allyl Amine to AN (Scheme 4)

Several ammonia molecules per allyl alcohol are desired at the active site domain for maximum AN yield (see Results section). The incorporation of nitrogen to form acrylonitrile via a route analogous to that in Scheme 2 but with substitution of Mo=NH for Mo=O is consistent with the results and is shown in Scheme 4. Initial chemisorption of ammonia with MoO_3 serves to block allyl alcohol chemisorption on oxidizing sites and results in formation of **10**. Reaction of **10** with allyl alcohol gives **11**, which upon Cope rearrangement, similar to the **4**-1,1-d_2/**4**-3,3-d_2 rearrangement (Scheme 2), gives σ-bonded N-allyl intermediate **12** as shown in Scheme 4. If only one ammonia molecule per alcohol site is

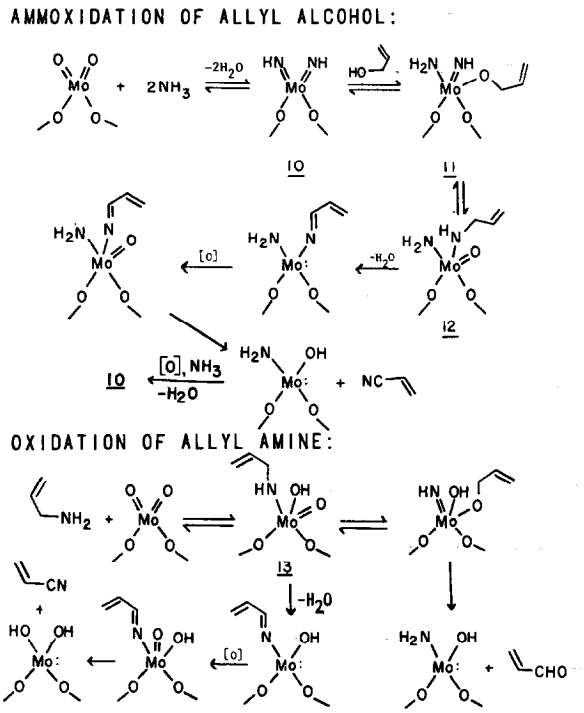

SCHEME 4. Acrylonitrile formation from reaction of allyl alcohol or allyl amine with MoO_3.

present, one of the NH groups in **11** would be replaced by O, and thus there would be a greater probability of forming acrolein. This is consistent with the oxidation of allyl amine, which initially produces σ-bond N-allyl species **13**. This intermediate can form either N- or O-inserted products as shown in Scheme 4, since both nitrogen and oxygen are bonded to the molybdenum in **13**. Hydrolysis of the imine formed from **13** could also contribute to acrolein formation.

Mechanistic Interpretation in Terms of Selective Propylene Oxidation (Scheme 5)

The molybdenum(VI) esters **4**, **5**, and **6** [Eqs. (3)–(5)] generated from allyl alcohol are analogous to the proposed allylic intermediates **3** [Eq. (2)] and **14** (Scheme 5) in the selective oxidation of propylene (*10, 11, 13*). The results are interpreted in terms of the formation of this intermediate by initial chemisorption on Mo centers, followed by allylic abstraction by Bi oxygens giving π-allyl intermediate **15**, which then collapses to form σ-complex **14**, the acrolein precursor. The incorporation of nitrogen in ammoxidation to form acrylonitrile is analogous to that depicted in Scheme 4 and involves formation of a σ-bonded N-allyl complex from an O-allyl species after catalyst N-incorporation via condensation of surface Mo=O double bonds with ammonia. Formation of AN results from two subsequent hydrogen abstraction reactions from this N-allyl complex as depicted in Scheme 5.

A comparison of this proposed selective oxidation mechanism with three other important mechanisms in the literature is shown in Table 11. There is a considerable amount of discrepancy here between the assignment of the role of the individual elemental components of the catalyst. Matsurma's results, based on low-temperature adsorption studies, attributes chemisorption and first hydrogen abstraction to Mo, while in Haber's mechanism, based on *in situ* generation of the allylic intermediate, the roles are reversed. Sleight, on the other hand, attributes all the steps shown here to MoO_4^{2-} groups, while the bismuth

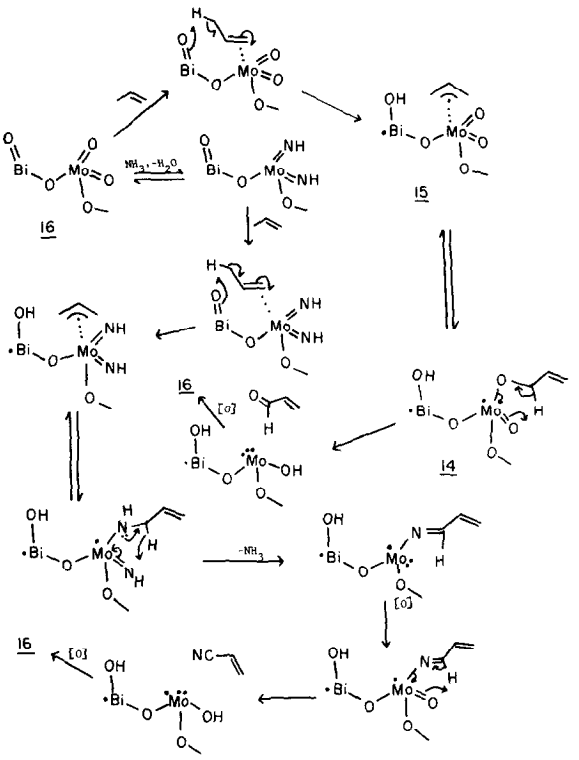

SCHEME 5. Mechanism for selective oxidation and ammoxidation of propylene over bismuth molybdate.

supplies an overlapping Bi/Mo conduction band ($6p/4d$), which serves as an electron sink. Our mechanism is based on a consideration of the reactions of both propylene and the allylic intermediate studied in this work by *in situ* generation from allyl alcohol. The former contains information concerning the initial chemisorption and the first α-hydrogen abstraction, while the latter is important in understanding subsequent steps.

CONCLUSIONS

In this work we have presented evidence that the reaction of allyl alcohol with MoO_3 and $Bi_2O_3 \cdot nMoO_3$ ($n = 1, 3$) occurs via

TABLE 11

Selective Oxidation Mechanism Comparisons

Step	Matsuura	Haber	Sleight	Grasselli *et al.*
Olefin chemisorption	Mo (B site)	Bi	Mo	Mo
NH_3 chemisorption, NH formation	Mo (B site)	Mo	Mo	Mo
1st allylic H abstraction	Mo (B site)	Bi	Mo	Bi
2nd (3rd) H abstractions	Mo (B site)	Mo	Mo	Mo
O(NH) insertion	Bi (A site)	Mo	Mo	Mo
Electron flow	$e^- \rightarrow$ Bi $\rightarrow$ Mo $\rightarrow O_2$	$e^- \rightarrow$ Mo $\rightarrow$ Bi $\rightarrow O_2$	$e^- \rightarrow$ Mo $\rightarrow$ Bi $\rightarrow O_2$ (also Keulks)	$e^- \rightarrow$ Mo $\rightarrow$ Bi $\rightarrow O_2$
Remarks	Site density (B) = 2× site density (A) A, high ΔH ads. B, low ΔH ads.	If no Mo present, C_6H_{10} forms from 2 allyls.	Bi_{6p}/Mo_{4d} overlap serves as e^- sink.	Bi facilitates 2nd/3rd H abstractions by e^- sink effect.

chemisorption on two types of sites: oxidation sites, on which acrolein is formed via allyl molybdates, and Brønsted acid sites, which form diallyl ether via allyl carbonium ion. Bismuth enhances the rate of α-hydrogen abstractions, the rate-determining step in allyl alcohol oxidation to acrolein. The extent of the C-1/C-3 interconversion in the isomeric deuterium-labeled allyl molybdates generated from allyl alcohol-1,1-d_2 and -3,3-d_2 is consistent with the formation of an analogous σ O-allyl molybdate (the acrolein precursor) via π-allyl molybdate in the selective oxidation of propylene. In ammoxidation, nitrogen incorporation occurs via a similar C-1/C-3 interconversion process on a surface in which surface Mo=O are replaced by Mo=NH. Thus, oxygen or nitrogen insertion prior to the second hydrogen abstraction is a likely mechanism in the selective oxidation and ammoxidation of propylene.

ACKNOWLEDGMENTS

The authors acknowledge Dr. K. L. Gallaher and Dr. J. Shen of The Standard Oil Company (Ohio) for their assistance in NMR and mass spectroscopy analyses.

REFERENCES

1. Dadyburjor, D. B., Jewur, S. S., and Ruckenstein, E., *Catal. Rev.* **19,** 293 (1979); Bielanski, A., and Haber, J., *Catal. Rev.* **19,** 1 (1979); Gates, B. C., Katzer, J. R., and Schuit, G. C. A., "Chemistry of Catalytic Processes," pp. 325–389. McGraw–Hill, New York, 1979, Hucknall, D. J., "Selective Oxidation of Hydrocarbons," p. 24 ff and references therein. Academic Press, New York, 1977.
2. Sachtler, W. M. H., and deBoer, N. H., *in* "Proceedings, 3rd International Congress on Catalysis, Amsterdam, 1964," p. 252. Wiley, New York, 1965; Adams, C. R., and Jennings, T., *J. Catal.* **2,** 63 (1963); Adams, C. R., and Jennings, T., *J. Catal.* **3,** 549 (1964); Adams, C. R., Voge, H. H., Morgan, C. Z., and Armstrong, W. E., *J. Catal.* **3,** 379 (1964); Grasselli, R. K., and Suresh, D. D., *J. Catal.* **25,** 273 (1972).
3. Keulks, G. W., and Krenzke, L. D., *in* "Proceedings, 6th International Congress on Catalysis, London, 1976" (G. C. Bonds, P. B. Wells, and F. C. Tompkins, Eds.), p. 806. The Chemical Society, London, 1977. Keulks, G. W., *J. Catal.* **19,** 232 (1970); Wragg, R. D., Ashmore, P. G., and Hockey, J. A., *J. Catal.* **22,** 49 (1971); Hoefs, E. V., Monnier, J. R., and Keulks, G. W., *J. Catal.* **57,** 331 (1979).
4. Sancier, K. M., Wentrcek, P. R., and Wise, H., *J. Catal.* **39,** 141 (1975).
5. Otsubo, T., Miura, H., Morikawa, Y., and Shirasaki, T., *J. Catal.* **36,** 240 (1975); Miura, H., Otsubo, T., Shirasaki, T., and Morikawa, Y., *J. Catal.* **56,** 84 (1979).
6. Mars, P., and van Krevelen, D. W., *Chem. Eng. Sci. Suppl.* **3,** 41 (1954); Dadyburjor, D. B., and Ruckenstein, E., *J. Phys. Chem.* **82,** 1563 (1978).
7. Giordano, N., Meazza, M., Castellan, A., Bart, J. C. J., and Ragaini, V., *J. Catal.* **50,** 342 (1977); Sancier, K. M., Dozono, T., and Wise, H. *J. Catal.* **23,** 270 (1971); Peacock, J. M., Sharp, M. J., Parker, A. J., Ashmore, P. G., and Hockey, J. A., *J. Catal.* **15,** 379 (1969).
8. Hart, P. J., and Friedli, H. R., *J. Chem. Soc. D,* 621 (1970).
9. Orlov, A. N., and Gagarin, S. G., *Kinet. Catal.* **15,** 1308 (1974); Callahan, J. L., Grasselli, R. K., Milberger, E. C., and Strecker, H. A., *Ind. Eng. Chem. Prod. Res. Develop.* **9,** 134 (1970)
10. Weiss, F., Marion, J., Metzger, J., and Cognion, J.-M. *Kinet. Catal.* **14,** 32 (1973).
11. Trifiro, F., Centola, P., Pasquon, I., and Jiru, P., *in* "Proceedings 4th International Congress on Catalysis, Moscow, 1968" (B. A. Kazansky, Ed.), p. 310. Adler, New York, 1968; Trifiro, F., and Pasquon, I., *J. Catal.* **12,** 412 (1968).
12. (a) Davydov, A. A., Mikhaltchenko, V. G., Sokolovskii, V. D., and Boreskov, G. K., *J. Catal.* **55,** 299 (1978); (b) Iwasawa, Y., Nakano, Y., and Ogasaware, S., *Trans. Faraday Soc. I,* **74,** 2968 (1978).
13. Burrington, J. D., and Grasselli, R. K., *J. Catal.* **59,** 79 (1979).
14. Grasselli, R. K., and Hardman, H. F., U.S. Patent 3,642,930 (Feb. 15, 1972); Grasselli, R. K., Miller, A. F., and Hardman, H. F., Ger. Offen. 2,147,480 (May 4, 1972); Grasselli, R. K., Miller, A. F., and Hardman, H. F., Ger. Offen. 2,203,709 (Aug. 17, 1972).
15. McMichael, K. D., *J. Amer. Chem. Soc.* **89,** 2943 (1967).
16. Schuetz, R. D., and Millard, F. W., *J. Org. Chem.* **24,** 297 (1959).
17. Murty, A. N., and Curl, R. F., Jr., *J. Chem. Phys.* **46,** 4176 (1967).
18. Brazdil, J. F., Suresh, D. D., and Grasselli, R. K., *J. Catal.* in press.